Soil Biology & Biochemistry 107 (2017) 133–143

Contents lists available at ScienceDirect

Soil Biology & Biochemistry

journal homepage: www.elsevier.com/locate/soilbio

Differences in soluble organic carbon chemistry in pore waters sampled from different pore size domains

V.L. Bailey [a, *], A.P. Smith [a], M. Tfaily [b], S.J. Fansler [a], B. Bond-Lamberty [c]

[a] Biological Sciences Division, Pacific Northwest National Laboratory, 99354 Richland, Washington, USA
[b] Environmental and Molecular Sciences Laboratory, Pacific Northwest National Laboratory, 99354 Richland, Washington, USA
[c] PNNL-University of Maryland Joint Global Climate Change Research Institute, College Park, 20740 Maryland, USA

ARTICLE INFO

Article history:
Received 13 April 2016
Received in revised form
22 November 2016
Accepted 26 November 2016
Available online 11 January 2017

Keywords:
Pore water
Carbon protection
Soil organic carbon
Soil structure
Decomposability

ABSTRACT

Spatial isolation of soil organic carbon (SOC) in different sized pores may be a mechanism by which otherwise labile carbon (C) could be protected in soils. When soil water content increases, the hydrologic connectivity of soil pores also increases, allowing greater transport of SOC and other resources from protected locations, to microbially colonized locations more favorable to decomposition. The heterogeneous distribution of specialized decomposers, C, and other resources throughout the soil indicates that the metabolism or persistence of soil C compounds is highly dependent on short-distance transport processes. The objective of this research was to characterize the complexity of C in pore waters held at weak and strong water tensions (effectively soil solution held behind coarse- and fine-pore throats, respectively) and evaluate the microbial decomposability of these pore waters. We saturated intact soil cores and extracted pore waters with increasing suction pressures to sequentially sample pore waters from increasingly fine pore domains. Ultrahigh resolution mass spectrometry of the SOC was used to profile the major biochemical classes (i.e., lipids, proteins, lignin, carbohydrates, and condensed aromatics) of compounds present in the pore waters; some of these samples were then used as substrates for growth of *Cellvibrio japonicus* (DSMZ 16018), *Streptomyces cellulosae* (ATCC® 25439™), and *Trichoderma reseei* (QM6a) in 7 day incubations. The soluble C in finer pores was more complex than the soluble C in coarser pores, and the incubations revealed that the more complex C in these fine pores is not recalcitrant. The decomposition of this complex C led to greater losses of C through respiration than the simpler C from coarser pore waters. Our research suggests that soils that experience repeated cycles of drying and wetting may be accompanied by repeated cycles of increased CO_2 fluxes that are driven by i) the transport of C from protected pools into active, ii) the chemical quality of the potentially soluble C, and iii) the type of microorganisms most likely to metabolize this C.

1. Introduction

The spatial separation of substrate, microbes, and extracellular activity is an important mechanism of soil organic carbon (SOC) protection in soils. Spatial isolation of SOC in different sized pores may be a mechanism by which otherwise labile carbon (C) could be protected in soils (Jastrow et al., 2007). This mechanism has already been attributed to protecting otherwise labile nitrogen (N) in Arctic tussock soils, where over half of the labile N was calculated to be neither sorbed nor mobile (Darrouzet-Nardi and Weintraub, 2014). Such physical isolation of potentially labile C is intriguing, but the wide spectrum of complex organic C molecules in soil makes it difficult to extrapolate these observations to SOC. Determining if spatial isolation in soil pores results in distinctly different C chemical profiles is a first step to determining the vulnerability of this protected C. When soils are saturated, all pore channels are filled with water and SOC and other nutrient resources can mix with microorganisms through diffusion and transport. As soils dry, these hydrologic connectivities through the soil matrix reduce, and some pores become relatively isolated from these transport processes. Reduced hydrologic connectivity of soil pores can increase the bacterial diversity in soils due to limited competition that

* Corresponding author. Pacific Northwest National Laboratory, 902 Battelle Boulevard, MSIN J4-18, 99352 Richland, Washington, USA.
E-mail addresses: vanessa.bailey@pnnl.gov (V.L. Bailey), peyton.smith@pnnl.gov (A.P. Smith), malak.tfaily@pnnl.gov (M. Tfaily), sarah.fansler@pnnl.gov (S.J. Fansler), bondlamberty@pnnl.gov (B. Bond-Lamberty).

http://dx.doi.org/10.1016/j.soilbio.2016.11.025

would normally reduce community diversity (Carson et al., 2010). Bacterial motility and resource diffusion are greatly reduced in soils at low matric potential that are dominated by thin water films, rather than saturated pores (Chowdhury et al., 2011). As soil moisture increases, the size of the labile C pool increases, inferred from fitted first- and zero-order kinetic models of soil respiration data (Bouckaert et al., 2013). Additionally, both the labile C pool size and the slow C pool mineralization rate increase with decreasing soil bulk density, i.e. increased total pore volume. There is evidence for an optimum balance between moisture and oxygen availability (Strong et al., 2004; Moyano et al., 2013) resulting in increased gas fluxes during soil wetting; additionally, the Birch effect of a significant respiration pulse following rewetting (Birch, 1958) may derive from the transport of occluded C to microbially active locations (Moyano et al., 2013). In the Birch effect, increased ionic strength due to drying can i) result in local osmotic stress lysing sensitive microorganisms (Moyano et al., 2013) and ii) changes to the chemical forms of C desorbed from soils under different ionic strengths (Mouvenchery et al., 2016). In the event that new C is mobilized through either process, pulses of soil moisture serve to facilitate the transport of this C from the protected location to microbially active sites, resulting in the Birch pulse of CO_2 (Lawrence et al., 2009; Parker and Schimel, 2011). This suggests that overall soil water distribution is a major driver for where C mineralization reactions occur in soils; ideal conditions may be found in finer pores surrounded by air-filled coarser pores (Bouckaert et al., 2013), or otherwise at the gas-water interface (Strong et al., 2004).

In studies of C decomposition at different matric potentials, the fastest decomposition of freshly added litter occurred in soils that were dominated by pore throats between 15 and 60 μm in diameter, and most slowly in soils with an abundance of pores with throat diameters <4 μm (Strong et al., 2004). However, this decomposition focused on freshly added C (Strong et al., 2004). Evaluating the C chemistry in native soils is intriguing because evidence suggests that soil C occurs as heterogeneously distributed "hotspots" throughout the soil, and that clear patterns of distribution do not exist for organic C chemical classes, other than the association of aliphatic and carboxylic compounds with clay mineral surfaces (Lehmann et al., 2007). Additionally, no consistent relationships between organic chemical class with soil residence time has been reported (Schmidt et al., 2011), suggesting that chemical composition doesn't limit decomposability. Thus, while "aged" or "weathered" soil C is often considered to be stable, under different moisture and temperature conditions this "stable" C will mobilize (Stutter et al., 2007). As C moves from protected locations, diffusion and decomposition processes make it difficult to predict the final spatial disposition of the solubilized C.

The objective of this research was to characterize the chemical composition of C in pore waters held at weak and strong water tensions (effectively soil solution held behind coarse- and fine-pore throats, respectively) and evaluate the microbial decomposability of the C dissolved in these pore waters. We hypothesized that the soluble C in these two pore domains would differ significantly from one another, with more condensed, aromatic SOC located in the finer pore domains because partially saturated conditions would isolate fine pores from the diverse microbial communities capable of decomposing these substrates. We also hypothesized that the chemical nature of the SOC in the pore waters would control its decomposition potential, with a fungal inoculant better able to deplete complex compounds (such as lignin and tannins) compared to the bacterial inoculants due to the differences in the metabolic potential of each microorganism. We tested these hypotheses in soils sampled across three locations within a hydrologic gradient at DWP, and at three soil depths. We studied intact soil cores collected from the Disney Wilderness Preserve (DWP), FL, USA. Water dynamics in this system, particularly water table rise and fall, influence the inputs and disposition of organic C at the surface and also at depth, making the DWP soils a good test case for examining how soil matrix accessibility, hydrologic connectivity, and decomposition potential are related.

2. Materials and methods

2.1. Soils

Intact soil cores (10 cm diameter, 30 cm height) were sampled from three locations across the Disney Wilderness Preserve (Orlando, FL) in June 2013. Soils at DWP are dominated by sandy textures, and depending on local topographic position show moderate to high levels of organic matter accumulation at the surface. The three locations were a drier pine flatwood stand where the soil was an Immokalee Series, sandy, siliceous, hyperthermic Arenic Alaquod (28.104641°, −81.419027°); an intermittent marsh composed of a Basinger fine sand, depressional (28.105535, −81.418896); and a wet "supermarsh" (28.099252, −81.417913) where the soil was a Floridana mucky fine sand, depressional. Soil cores were sampled from 0 to 30 cm, 30–60 cm, and 60–90 cm depth intervals from the same borehole. Four replicates of each set of sequential cores were sampled from each of the three locations, randomly located and separated by 2–5 m. Physical and chemical properties of the soils used in this study are included as Supplemental Table 1. Soils were placed on blue ice, and transported back to the University of Central Florida (Orlando, FL, USA), where they were placed in a freezer at −20 for 48 h in order to comply with USDA-APHIS regulations controlling transport of soil from a fire ant quarantine area, before being shipped to Pacific Northwest National Lab (Richland, WA, USA). Once received at PNNL, soils were stored at 4 °C prior to conditioning and saturation.

2.2. Pore water sampling

Soils were conditioned in the lab at room temperature (21 °C), and allowed to freely imbibe water from the bottom through a saturated porous ceramic plate (Soil Moisture Equipment Corp., Goleta, CA, USA). Cores were incubated under these conditions for 72 h. Pore waters were sampled by transferring each core onto individual 100 kPa Tempe Pressure Cell units fit with a high flow ceramic plate (Soil Moisture Equipment Corp. Goleta, CA, USA) to sequentially collect pore waters with suctions of −1.5 kPa, then −15 kPa, and finally, −50 kPa using a pump with a PCD Dual Valve pressure controller (Alicat Scientific, Tuscon, AZ). The ceramic pore plates have a pore size diameter of 2.5 μm, effectively removing particulates and some of the bacteria from the pore water. Pore water was collected into borosilicate vials for 24 h, or until flow ceased at a given suction, at each suction setting and stored at −20 °C until analysis. In this manuscript, pore water fractions will be identified by their sampling suctions. Preliminary tests indicated that the duration of suction had no effect on SOC composition.

The Kelvin equation for perfectly wettable soils can be used to estimate the largest water-filled pore diameter at a given water potential (Marshall and Holmes, 1996). It can be reduced to:

$$\text{largest water filled pore diameter } (\mu m) = \frac{300}{\textit{water potential } (kPa)}$$

Using the Kelvin equation (Marshall and Holmes, 1996; Carson

et al., 2010) as a rough estimate of the largest water-filled pore diameter, the sampling suctions given above correspond to ~200 μm, 20 μm, and 6 μm, respectively.

2.3. Organic matter characterization

Ultrahigh resolution characterization of dissolved organic carbon (DOC) was carried out using a 12 Tesla Bruker SolariX Fourier transform ion cyclotron resonance (FT-ICR) mass spectrometer (MS) located at the Environmental Molecular Sciences Laboratory (EMSL), a Department of Energy- Office of Biological and Environmental Research national user facility in Richland, WA, USA. Samples were diluted 1:1 (v/v) with LC-MS grade methanol. This dilution was conducted less than half an hour before analyzing the samples to minimize potential esterification of the DOC by methanol. Samples were then injected directly into the mass spectrometer and the ion accumulation time was optimized for all samples. A standard Bruker electrospray ionization (ESI) source was used to generate negatively charged molecular ions. Samples were introduced to the ESI source equipped with a fused silica tube (30 μm i.d.) through an Agilent 1200 series pump (Agilent Technologies) at a flow rate of 3.0 μL min^{-1}. Experimental conditions were as follows: needle voltage, +4.4 kV; Q1 set to 50 *m/z*; and the heated resistively coated glass capillary operated at 180 °C. These were optimal parameters established in earlier dissolved organic carbon characterization experiments (Tfaily et al., 2015).

Ninety-six individual scans were averaged for each sample and internally calibrated using an organic matter homologous series separated by 14 Da ($-CH_2$ groups). The mass measurement accuracy was less than 1 ppm for singly charged ions across a broad *m/z* range (100–1100 *m/z*). The mass resolution was ~350 K at 339 m/z. Data Analysis software (BrukerDaltonik version 4.2) was used to convert raw spectra to a list of m/z values ("features") applying FTMS peak picker with a signal-to-noise ratio (S/N) threshold set to 7 and absolute intensity threshold to the default value of 100. Chemical formulae were then assigned using an in-house built software following the Compound Identification Algorithm (CIA), described by (Kujawinski and Behn, 2006) and modified by (Minor et al., 2012). Chemical formulae were assigned based on the following criteria: S/N > 7, and mass measurement error <1 ppm, taking into consideration the presence of C, H, O, N, S and P and excluding other elements.

To interpret the resulting large data set, the chemical character of all of the data points for each sample spectrum was evaluated on van Krevelen diagrams generated from the ESI FT-ICR MS mass spectra (Fenn et al., 1989). Peaks were assigned on the van Krevelen diagram on the basis of their molar H:C ratios (y-axis) and molar O:C ratios (x-axis). Van Krevelen diagrams provide a means to visualize and compare the average properties of OM and enable identification of the major biochemical classes (i.e., lipids, proteins, lignin, carbohydrates, and condensed aromatics) of compounds present in samples. It is important to note that in Van Krevelen diagrams, molecules with different molecular formulas will plot at the same point if their H:C and O:C ratios coincide (Sleighter and Hatcher, 2007; Tfaily et al., 2015). Biochemical compound classes are reported as relative abundance values based on counts of C, H, and O for the following H:C and O:C ranges; lipids ($0 < O{:}C \leq 0.3$, $1.5 \leq H{:}C \leq 2.5$), unsaturated hydrocarbons ($0 \leq O{:}C \leq 0.125$, $0.8 \leq H{:}C < 2.5$), proteins ($0.3 < O{:}C \leq 0.55, 1.5 \leq H{:}C \leq 2.3$), amino sugars ($0.55 < O{:}C \leq 0.7$, $1.5 \leq H{:}C \leq 2.2$), carbohydrates ($0.7 < O{:}C \leq 1.5$, $1.5 \leq H{:}C \leq 2.5$), lignin ($0.125 < O{:}C \leq 0.65$, $0.8 \leq H{:}C < 1.5$), tannins ($0.65 < O{:}C \leq 1.1$, $0.8 \leq H{:}C < 1.5$), and condensed hydrocarbons ($0 \leq O{:}C \leq 0.95$, $0.2 \leq H{:}C < 0.8$). Unnamed compounds are calculated as the proportion of identified C that does not fit within the above defined H:C and O:C ranges (Sleighter and Hatcher, 2007; Tfaily et al., 2015). To describe the thermodynamic reactivity of each compound, the stoichiometry of each assigned formula was used to calculate the nominal oxidation state of C (NOSC) for that compound (LaRowe and Van Cappellen, 2011). NOSC of individual compounds present in each sample was averaged to give the mean NOSC of soluble organic matter in that sample. The aliphatic-to-aromatic ratio was calculated based a modified aromaticity index (AI_{mod}) calculated as $(1 + C - ½\,O - S - ½\,H)/(C\text{-}1/2\,O - S - N - P)$ where aromatic compounds are $AI_{mod} > 0.5$ and aliphatic compounds consist of H:C values between 1.5 and 2.0, as defined in Chassé et al., (2015).

To identify potential microbial metabolic pathways, the mass difference between m/z peaks extracted from each spectrum with S/N > 7 were compared to commonly observed mass difference for common metabolic transformations (Breitling et al., 2006). This is possible because, in addition to offering putative identification of formulas, FT-ICR MS has the potential to identify the structural link between related organic compounds, since chemically transformed species will be related by measurable, clearly defined mass differences. In this approach, all pairwise mass–mass differences were calculated for each dataset. The observed pairwise mass–mass differences were then compared to a list of 83 mass differences corresponding to common metabolic reactions. Here, pairs of compounds whose mass difference matched the expected amount (within 1 ppm) were considered to be related by the corresponding metabolic transformation.

Concentrations of total C and N in pore water were determined via combustion catalytic oxidation method using a Shimadzu TOC-5000A TOC analyzer (Shimadzu, Columbia, MD, USA) located at EMSL.

2.4. Inoculae and incubation

Select common soil bacteria from pure cultures, *Cellvibrio japonicus* (DSMZ 16018) and *Streptomyces cellulosae* (ATCC® 25439™) were grown in minimal media (MR-1) that was increasingly diluted with filter-sterilized pore water (a pooled sample of the −15 kPa pore waters) over the course of one month. Cell concentration and bacterial growth phases were determined via optical density readings at 600 nm wavelengths via a Bioscreen-C (Oy Growth Curves Ad Ltd, Raisio, Finland). The fungal inoculant, wild-type *Trichoderma reseei* (QM6a), was cultivated on solid potato dextrose agar (BD Difco, Franklin Lakes, New Jersey, USA). After 2 weeks, conidia were collected, stored in sterile distilled (DI) water and then enumerated using a haemacytometer prior to sexual germination. Inoculants were chosen based on a variety of factors, such as, they all exhibited a high growth capability in the laboratory, they all are common soil decomposers, each well-studied and –documented, and they are representative members of important soil microbial guilds; gram-negative bacteria, gram-positive actinobacteria and saprotrophic fungi (Moorhead and Sinsabaugh, 2006).

The incubation began when 100 μl of each pure-culture bacterial batch in exponential growth was added to individual vials containing filter-sterilized dilutions (1:5, pore water: DI) for a total volume of 5 ml of select subsamples of pore water sampled with −1.5 and −15 kPa (n = 5). Subsampling was based primarily on the volume of pore water available for each fraction, and to ensure that the pairs of pore water fractions (−1.5 and −15 kPa) were derived from the same core. Preliminary analyses showed a significant difference between the chemical compositions of the −1.5 kPa and −50 kPa pore waters; the chemical profiles of the −15 kPa samples were more variable. As the volumes of the −50 kPa fractions were small, and consumed mainly by the FT-ICR analyses, we deliberately selected −15 kPa pore waters for

which the FT-ICR profiles did not differ significantly from the −50 kPa fractions. Controls included filter-sterilized pore water in the absence of any microbial inoculant.

Static CO_2 concentrations were measured via manual injection using an EGM-4 (PP Systems, Amesbury, MA, USA). Calibration gas standards (Gasco Affiliates, LLC, Oldsmar, FL, USA) were used to verify measurement accuracy and precision throughout the incubation. Briefly, 5 ml of headspace gas was extracted from incubation vials through a 0.2 μm filter using a 5 ml locking, sterile syringe and injected into the EGM-4. CO_2 concentration (ppm) was recorded when values stabilized following the initial peak. Measurements were taken 2, 4, 8, 16, 24, 36, 48, 72, 96, 120, 14, 171, and 192 h following inoculation. Vials were evacuated every twenty-four hours after first 48 h of the incubation. Respiration was calculated as A = dC/dt * V/P * Pa/RT (Steduto et al., 2002), where A is the flux (μmol g^{-1} s^{-1}), dC/dt the change in measured CO_2-C concentrations as above (mole fraction s^{-1}), V the total system volume (cm^3), P the pore water volume (ml), Pa the atmospheric pressure (kPa), R the universal gas constant (8.3 × 10^3 cm^3 kPa mol^{-1} K^{-1}), and T air temperature (K).

Aliquots of the substrate prior to the incubation were taken for baseline measurements (C chemical composition and concentration. At the end of the incubation, 200 μl aliquots were used to measure the concentration of C and N and molecular composition using FT-ICR MS remaining in the inoculate pore waters (as described above). Differences in pre- and post-incubation FT-ICR profiles were measured using a relative change ratio equation, where the values are weighted abundances of the features comprising a given compound class:

$$\textit{Relative Change Ratio} = \frac{(\textit{post incubation value} - \textit{preincubation value})}{\textit{preincubation value}}$$

2.5. Statistical analyses

Non-metric multidimensional scaling (NMS) was performed on relative abundance of FT-ICR compound features (lipids, unsaturated hydrocarbons, proteins, amino sugars, tannins, carbohydrates, lignin, and condensed hydrocarbons) using PC-ORD 6 (MjM Software Design, Gleneden Beach, OR, USA).

Statistical analyses were performed using JMP Pro Version 12 (SAS Inst. Inc., Cary, NC, USA). Restricted maximum likelihood (REML) models were used to test the effects of soil depth (0–30, 30–60, 60–90 cm), location (dry pinewood flats, intermittent marsh, wet "supermarsh"), and effective pore size class (samples drawn with suctions of −1.5 kPa, −50 kPa) on C and N concentrations and on C compound classes determined via FT-ICR MS. Out of the 36 cores collected representing each site and depth at DWP (including 4 replicate cores), only 27 loosely held pore water samples (1.5 kPa) and 20 tightly held pore water samples (−50 kPa) were collected with volumes large enough to run FT-ICR measurements on (e.g. 0.5 ml). Preliminary data analysis using all samples of soil pore water collected at these two suctions revealed, surprisingly, no effect of soil depth or sampling location for any of the variables analyzed (Supplemental Fig. 1). Due to the unequal sampling size and high variability among cores, we chose to select of subset of paired −1.5 and −50 k Pa samples collected from the same core. This narrowed our samples down to 14 cores. Due to the continued absence of any effects of soil depth or sampling location, REML models were adjusted to test the sole effect of effective pore size class (i.e. suction). Any values transformed to meet normal distribution requirements of models are noted in figure captions. Correlations between variables, such as FT-ICR features and total C, were accepted as significant if the both the analysis of variance (ANOVA) and parameter estimates (both the intercept and x-variable) were significant ($p < 0.05$). The original soil core from which the pore water was extracted was included as a random variable to account for heterogeneity among cores (i.e. replicates). For the inoculated incubation, REML models included effective pore size class (−1.5 kPa, −15 kPa), inoculant type (*Cellvibrio japonicus*, *Streptomyces cellulosae, Trichoderma reseei*), and an interaction of effective pore size class and inoculant as fixed effects. Summarized data supporting the results and figures presented below are permanently archived and available at https://dx.doi.org/10.6084/m9.figshare.4240232.v1.

3. Results

3.1. -1.5 kPa versus −50 kPa

Nonmetric multidimensional scaling (NMS) was used to plot Bray-Curtis similarities of the pore waters sampled with the two different suctions (Fig. 1). A two-dimensional solution explained 87.9% of the variation observed in the FT-ICR MS data, with condensed hydrocarbons explaining 89.4% of the variation along axis 1, and lignin explaining 64.8% of the variation along axis 2 (Table 1). A third dimension in the NMS analysis would explain an additional 9.4% of the variation (not shown), but this separation is largely driven by unsaturated hydrocarbons (83.8%; Table 1). Axis 1 positively correlated with total C observed in pore waters ($p = 0.029$), whereas axis 2 positively correlated with both total C ($p = 0.012$) and N ($p = 0.015$). The more tightly held pore waters (i.e., retained by finer pore throats; −50 kPa) had greater relative abundances of condensed hydrocarbons, lignin and tannins compared to the more loosely held water (i.e., retained by coarser pore throats; −1.5 kPa), which had relatively more lipids (Table 2). These differences were consistent for all three transect positions, and all three soil depths. There were no differences by sampling location (site) or soil depth in NMS axes values (see Table 3).

The more tightly held pore waters also had a higher mean O:C (0.368 ± 0.011, $p = 0.0128$), lower H:C (1.167 ± 0.037, $p = 0.0036$) and a NOSC closer to zero (−0.124 ± 0.073, $p = 0.0165$) than the more loosely held pore waters (0.328 ± 0.009 O:C, 1.301 ± 0.019 H:C, and −0.356 ± 0.046 NOSC) (Fig. 2). There were no differences, however, in O:C, H:C and NOSC by sampling location (site), or soil depth.

The more tightly held pore waters contained more total C and N compared to the more loosely held pore waters (−1.5 kPa (Table 2). Differences in total C or N among soil cores ($n = 14$) made up 45.7% and 47.8%, respectively, of the estimated variance components. Total C and N were negatively correlated with the relative abundance of lipids in the pore waters ($p = 0.0007$ and $p = 0.0012$, respectively). Lipids were relatively enriched in more loosely held pore waters (−1.5 kPa) (Table 2). Total N was positively correlated with lignin ($p = 0.0059$) and tannins ($p = 0.0077$), all of which were greater in more tightly hold pore water (−50 kPa) (Table 2).

3.2. -1.5 kPa versus −15 kPa

For all model microorganisms, pore waters sampled with intermediate suction (−15 kPa) had greater CO_2 respiration rates ($p = 0.0061$) compared to the more loosely held pore water (−1.5 kPa), following an initial lag of ~80 h (Fig. 3). By the end of the incubation, more C was lost via CO_2 from pore waters held at an intermediate suction (−15 kPa) compared to the more loosely held pore water (−1.5 kPa) ($p = 0.0002$), averaged across inoculants. However, total CO_2-C losses differed among inoculants

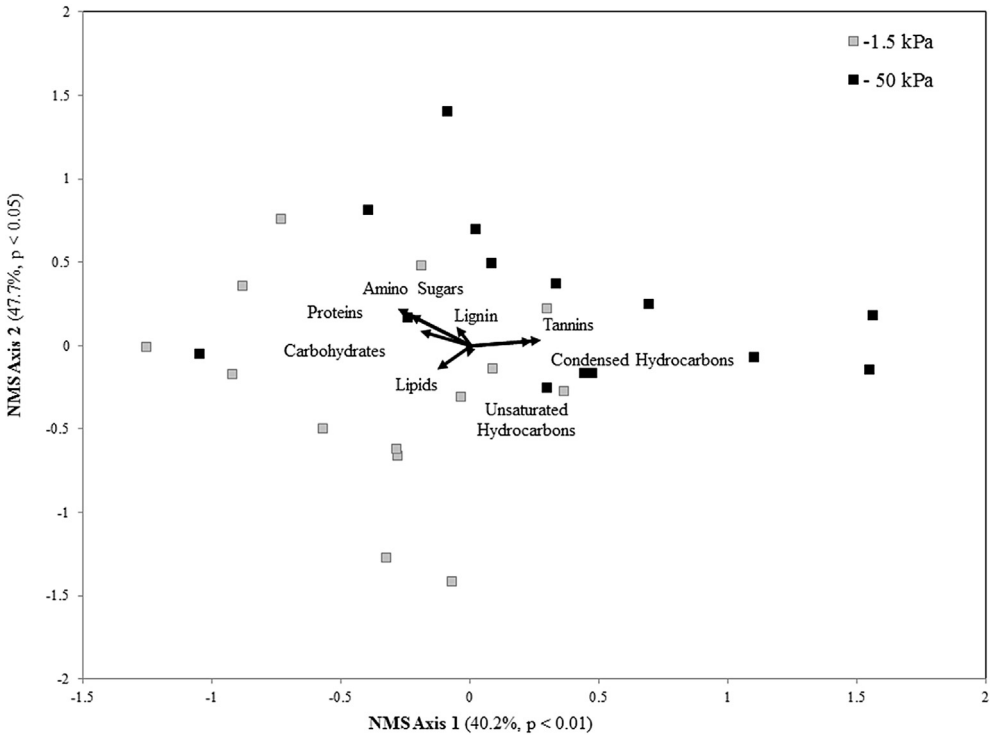

Fig. 1. Nonmetric multidimensional scaling (NMS) plot of Bray-Curtis similarities for Fourier Transform Ion Cyclotron Resonance (FT-ICR) compound classes in soil pore water collected at different suctions (−1.5 kPa, −50 kPa) showing 2 axes from a 3-axis solution (3rd axis not shown) with a final stress value of 5.134. Pore waters collected at −1.5 kPa are represented by light gray markers, whereas pore waters collected at −50 kPa are represented by black markers. Analysis of variance (ANOVA) was performed on separated pore water extracted at different suctions along Axis 1 ($p = 0.0067$) and Axis 2 ($p = 0.0224$) ($n = 14$).

($p < 0.0001$), with greater losses observed in *Trichoderma reesei*-inoculated pore waters (Fig. 4). Unlike the pore waters suctioned at −50 kPa reported in the above section (where $n = 14$), there was no difference in the concentration of C and N in the pore waters suctioned at −15 kPa and −1.5 kPa ($n = 5$). For the pore waters collected at −1.5 kPa used in the C-mineralization incubation experiment, the mean soluble C content was 133.09 ± 11.04 mg/L for total C, 74.8 ± 6.95 mg/L for organic C, with 6.59 ± 3.67 mg/L of N. For the pore waters suctioned at −15 kPa, the mean soluble C content was 167.26 ± 20.40 mg/L for total C, 103.01 ± 20.69 mg/L for organic C, with 5.55 ± 1.37 mg/L of N.

Even with differences in CO_2 respiration between pore water suctions, there were no differences in the aromatic-to-aliphatic ratio or FT-ICR compound classes (lipids, carbohydrates, condensed hydrocarbons, etc.) between pore waters held at the intermediate suction (−15 kPa) and pore waters loosely held (−1.5 kPa). Instead, differences in SOC transformations (i.e. changes in pre- and post-incubated FT-ICR profiles) were observed among inoculae. Changes in the overall aromatic-to-aliphatic ratio of FT-ICR identified features did not change (i.e. relative change ratio is statistically equal to zero) for most inoculae and pore water suctions, with the exception of *C. japonius* (Fig. 5, $p = 0.0004$). There were, however, relative increases or decreases in six of the eight defined FT-ICR compound classes pre- and post-incubation (Table 4), which differed by microbial inoculant. The effect of inoculant type significantly altered the relative abundance of lipids ($p = 0.0005$), proteins ($p = 0.0015$), unsaturated hydrocarbons

Table 1
Correlations with the nonmetric dimensional scaling ordination axes for plots of the Bray-Curtis similarities of pore waters sampled with −1.5 kPa and −50 kPa suctions.

Factor	Correlations with NMS ordination axes		
	Axis 1 (40.2%)	Axis 2 (47.7%)	Axis 3 (9.4%)
Lipid	0.34	0.57	0.06
Unsaturated hydrocarbons	0.00	0.09	0.84
Proteins	0.44	0.33	0.12
Lignin	0.11	0.65	0.10
Carbohydrates	0.36	0.11	0.01
Amino Sugars	0.38	0.32	0.01
Tannins	0.54	0.01	0.00
Condensed Hydrocarbons	0.89	0.02	0.03

Table 2
Mean and standard error values for Fourier Transform Ion Cyclotron Resonance (FT-ICR) compound classes and concentrations of dissolved carbon (C) and nitrogen (N) for soil pore water collected at different suctions (−1.5 and −50 kPa) ($n = 14$). Values listed for compound features are relative abundance values based on sum of all FT-ICR features observed included unnamed compounds (data not shown). C compounds that differ between different suctions are marked with an asterisk (*) based on REML model of each feature.

Carbon Properties	Pore Size Class-collected with tensions (kPa)	
	−1.5 kPa	−50 kPa
Compound Features (% of total sample)		
Lipids**	21.9 ± 1.6	14.8 ± 1
Unsaturated Hydrocarbons	9.5 ± 0.8	8.6 ± 1.1
Proteins	7.5 ± 1.3	6.7 ± 1.1
Lignin*	12.5 ± 0.8	14.2 ± 0.9
Carbohydrates	2.6 ± 0.3	1.9 ± 0.2
Amino Sugars	2.2 ± 0.3	1.6 ± 0.2
Tannins**	1.6 ± 0.2	2.8 ± 0.4
Condensed Hydrocarbons*	9.4 ± 0.6	13.5 ± 1.3
Dissolved Resources		
C (mg/L)***	71.4 ± 13.1	219.3 ± 28.0
N (mg/L)***	2.71 ± 0.48	8.41 ± 1.10

*$p < 0.05$, **$p < 0.005$, ***$p < 0.0001$.

Table 3
Model fit and summary statistics for Restricted Maximum Likelihood (REML) model for CO_2 respiration (mg CO_2-C ml^{-1} hr^{-1}, log transformed) from incubation with select microbial inoculae on soil pore water collected at −1.5 kPa and −15 kPa (cf. Fig. 2).

	df	SS	F ratio	Prob > F
Model	7	85.4	6.81	<0.0001
Model Effects				
Pore Water Suction (−1.5, −15 kPa)	1	9.35	7.60	0.023
Inoculae	3	74.96	20.29	<0.0001
Pore Size Class * Inoculae	3	1.06	0.29	0.898

df = degrees of freedom, SS = sum of squares, Prob > F = p-value.

($p < 0.0001$), carbohydrates ($p = 0.0070$), lignin (0.0061), and unnamed compounds ($p < 0.0001$) observed in the pore waters (Table 4). With the exception of lignin, *C. japonicus* varied from the other inoculae in the above mentioned compounds. We also observed differences between pre and post-incubation abundance in the greatest number of compound classes from *Cellvibrio japonicus*-inoculated pore water compared to other inoculae, such as relative decreases in lipids, proteins, unsaturated hydrocarbons, and lignin, with a relative increase in unnamed compounds (Table 4). *Streptomyces cellulosae*- and *Trichoderma reesei*-inoculated pore waters showed a relative increase in carbohydrates, whereas *Streptomyces cellulosae*-inoculated pore water also showed a relative depletion in lipids and proteins, while *Trichoderma reesei*-inoculated pore waters showed an additional relative increase in unsaturated hydrocarbons ($p < 0.05$ for all compounds and inoculae, Table 4).

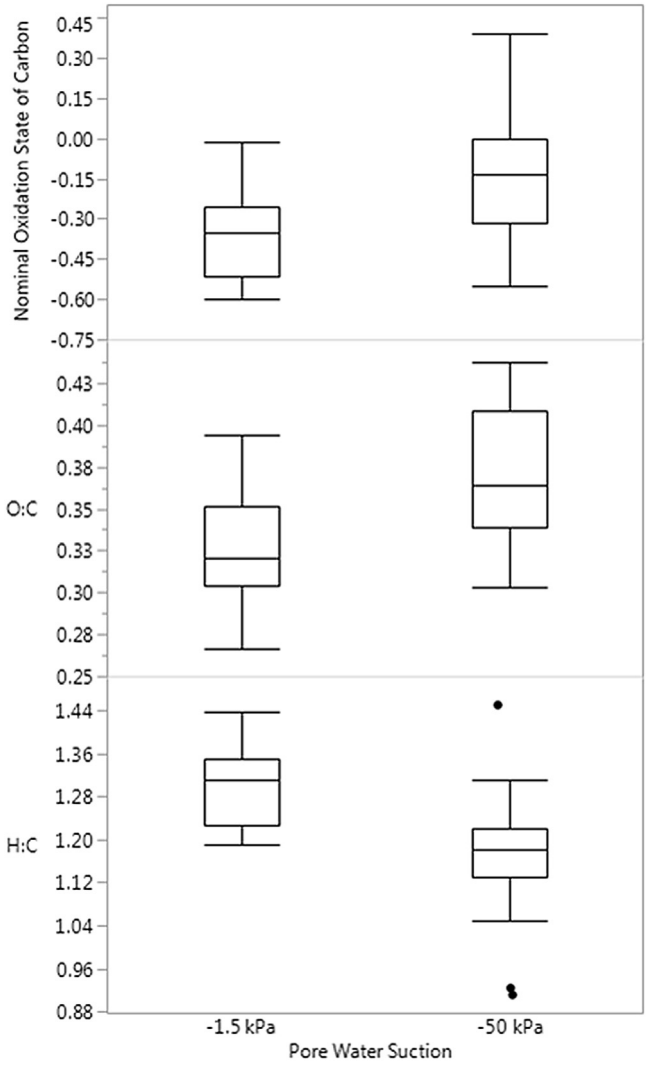

Fig. 2. Mean nominal oxidation state of C (NOSC), O:C and H:C identified with Fourier Transform Ion Cyclotron Resonance (FT-ICR) for soil pore water collected at different suctions (−1.5 kPa, 50 kPa). Pore water (suction) had a significant effect ($p < 0.05$) for all; NOSC, O:C and H:C.

When the relative change ratio of the FT-ICR compound classes for each inoculae was tested as being significantly different from zero (i.e. there was a change in the abundance between pre- and post-incubation compounds), we also saw striking differences between inoculae (values marked in bold in Table 4). We observed changes in the abundance of lipids and proteins in *C. japonicus*- and *S. cellulosae*-inoculated pore waters, unsaturated hydrocarbons and unnamed compounds in *C. japonicus*- and *T. reseei*-inoculated pore waters, carbohydrates in *S. cellulosae*-inoculated pore waters, and lignin in *C. japonicus* inoculated pore waters (Table 4). Even when FT-ICR profiles for each inoculant were analyzed individually, FT-ICR MS features from pore waters sampled with −1.5 kPa and −15 kPa did not differ. We did observe, however, differences in amino acid transformations between effective pore size classes (Table 5). Of the 84 different microbial metabolic pathways identified in our pore water samples, the 13 that differed between effective pore size classes were all amino acids (Table 5). For all inoculants, more amino acids transformations occurred in pore water held more loosely (−1.5 kPa) compared to the intermediately held pore waters (−15 kPa) (Table 5). In addition, we observed differences in 46 of 84 identified microbial transformation pathways among inoculants with the majority of changes occurring in *Streptomyces cellulosae*- or *Cellvibrio japonicus*-inoculated pore waters (Table 5, Supplemental Table 2).

4. Discussion

4.1. Differences in C chemistry with pore size

One of the challenges of this experiment was the use of individual, paired pore water samples, obtained from the same soil core. While pooling all of the pore waters of the same size fraction, then aliquoting them out as a uniform, representative sample of the pore waters of that size fraction might have provided a more homogeneous substrate and reduced some of the variability we detected within replicates, it would also not have been as reflective of the overriding heterogeneities that occur in soils at these scales. The incubated soil cores were relatively large, 10 cm in diameter and 30 cm deep. Spatial heterogeneities have however been observed in microbial community structure, as well as the C and N controls on their activities at scales ranging from 2.5 to 40 cm (Franklin and Mills, 2003, 2009). We have also observed significant variation in soil pore structures at scales approximating 100 μm (Bailey et al., 2013b) and in enzymatic activities at this scale (Bailey et al., 2012, 2013a). Because there is evidence that this patchy distribution of C, nutrients, and microbial activities affects predictions of net core-scale properties such as C mineralization (Manzoni et al., 2008), we deliberately avoided pooling the pore waters obtained from a size fraction from different cores; we sought to contain the influence of pore scale heterogeneity to an individual core. Furthermore, we treated each pore size class as discrete samples. However, the intrinsically connected nature of the soil pore network is such that the chemical profile of each sample may have been influenced by the collection method (i.e. as sample was drawn through pores and channels to the collection vial). Most of the chemical classes we used are inclusive of a range

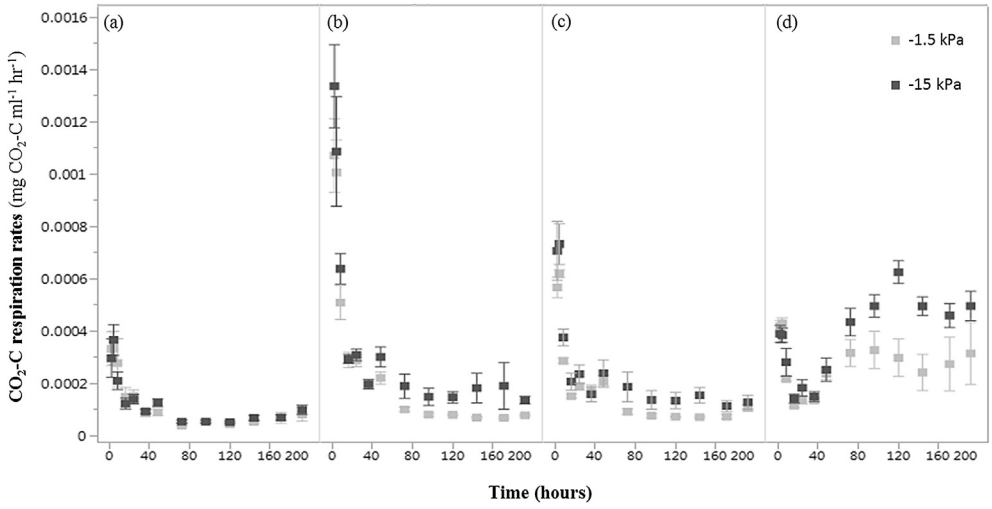

Fig. 3. Mean CO_2 respiration rates (mg CO_2 C ml^{-1} hr^{-1}) for (a) control (no inoculants), (b) *Cellvibrio japonicus*, (c) *Streptomyces cellulosae,* and (d) *Trichoderma reseei* for pore waters collected at −1.5 kPa (light gray markers) and −15 kPa (dark gray markers) over duration of incubation (200 min) (n = 5). Error bars represent 1 standard error from the mean. Inoculants *C. japonicus*, *S. cellulosae* and *T. reseei* stand for *Cellvibrio japonicus*, *Streptomyces cellulosae* and *Trichoderma reseei*, respectively.

of chemical traits (e.g. hydrophobic or hydrophilic compounds) and we, therefore, did not investigate biases towards select chemical traits in our pore water fractions.

In addition to the physical location of SOC, the chemical nature of the SOC in these different pore size domains is also a key characteristic needed to differentiate physical and chemical SOC protection mechanisms. To specifically describe the chemical quality of the SOC that could be solubilized and then transported from isolated or protected soil locations, we used ESI FT-ICR MS to examine differences in the chemical complexity of pore water held with different tensions. Recent applications of ESI FT-ICR MS to soils have shown with more detail the molecular complexity of SOC (Tfaily et al., 2015). This complexity includes over 4000 different C compounds (features) extracted by methanol from intact soils; ordinations of these compounds were able to differentiate four different soils. Our pore waters were similarly complex, in that over 2857 different C compounds were observed in the loosely held (−1.5 kPa) pore waters and 3226 different were counted in the more tightly held (−50 kPa) pore waters. Furthermore, it is notable that despite differences between sites or with depth observed in the physical and chemical properties of the soil cores (Supplemental Table 1), these differences were not reflected in the molecular profiles of soluble SOC located in the soil pore water.

Our samples from soil pores larger than ~6 μm in diameter were dominated by lipids and other broadly decomposable C substrates.

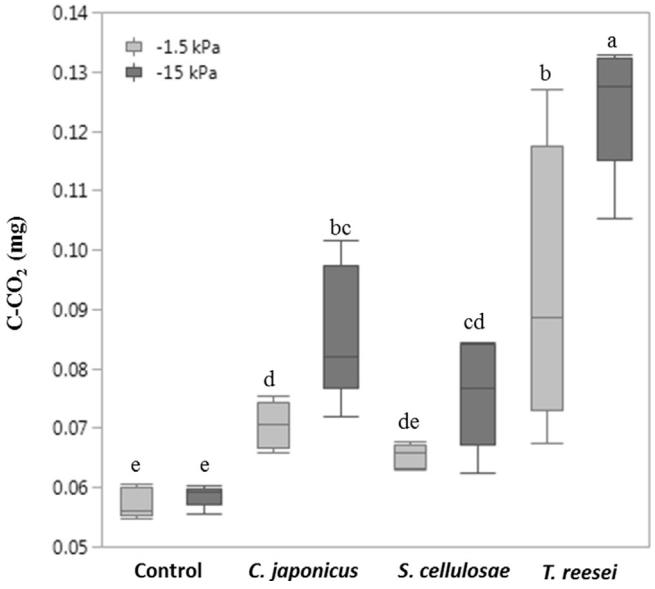

Fig. 4. Mean cumulative CO_2-C losses over duration of incubation (200 h) for each inoculant, including control for pore waters collected at −1.5 kPa (light gray box columns) and −15 kPa (dark gray box columns) (n = 5). Letters not shared across box columns indicate significant mean differences calculated using Student's mean comparison test. Inoculants *C. japonicus*, *S. cellulosae* and *T. reseei* stand for *Cellvibrio japonicus*, *Streptomyces cellulosae* and *Trichoderma reseei*, respectively.

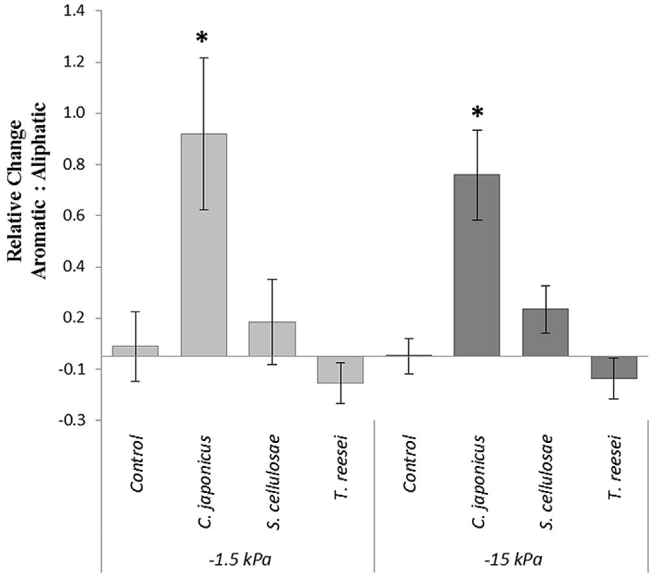

Fig. 5. The relative change ratio of aromatic-to-aliphatic compounds for each inoculant and pore water suction. Letters not shared across box columns indicate significant mean differences calculated using Student's mean comparison test. An asterisk (*) next to the letter means that the relative change ratio of aromatic-to-aliphatic compounds was significantly different from zero (i.e. there was a change pre- and post-incubation). Inoculants *C. japonicus*, *S. cellulosae* and *T. reseei* stand for *Cellvibrio japonicus*, *Streptomyces cellulosae* and *Trichoderma reseei*, respectively.

Table 4
Mean and standard error of relative change ratios for FT-ICR compounds (n = 5). Letters not shared across rows indicate significant mean differences between inoculae calculated using Student's mean comparison test. Values in bold are significantly different from zero (i.e. relative abundance of compound changed over course of incubation).

	Lipids	Proteins	Unsaturated Hydrocarbons	Amino Sugars	Carbohydrates	Condensed Hydrocarbons	Tannins	Lignin	Unnamed Compounds
Control (no inoculant)	−0.049 ± 0.109 **ab**	−0.163 ± 0.106 **a**	−0.018 ± 0.073 **b**	0.066 ± 0.155	0.242 ± 0.117 **a**	0.091 ± 0.143	0.094 ± 0.27	−0.091 ± 0.105 **bc**	0.025 ± 0.03 **b**
Cellvibrio japonicus	** **-0.414 ± 0.077 c**	** **-0.483 ± 0.084 b**	*** **-0.406 ± 0.045 c**	0.446 ± 0.771	−0.161 ± 0.088**b**	−0.045 ± 0.115	0.288 ± 0.196	* **-0.216 ± 0.081 c**	** **0.173 ± 0.032 a**
Streptomyces cellulosae	*0.084 ± 0.097 **bc**	* **-0.089 ± 0.88 a**	0.223 ± 0.053 **b**	1.799 ± 1.391	*0.459 ± 0.159 **a**	0.283 ± 0.151	0.329 ± 0.242	0.282 ± 0.136 **ab**	−0.081 ± 0.03 **b**
Trichoderma reesei	−0.243 ± 0.114 **a**	−0.179 ± 0.077 **a**	** **-0.151 ± 0.077 a**	1.109 ± 0.785	*0.748 ± 0.368 **a**	−0.031 ± 0.061	0.257 ± 0.226	0.211 ± 0.23 **a**	*0.047 ± 0.047 **c**

*p < 0.05, **p < 0.005, ***p < 0.0001.

In contrast, it is intriguing that the finer, less accessible pores contained relatively greater proportions of nominally complex C (lignins, tannins) than the larger pores. Differences in C composition between pores of different sizes and connectedness may be expected as macroaggregates and well-connected, coarse-sized pores would be generally enriched in more labile, fresh litter substrates, rich in lipid-like compounds, compared to substrates occluded within microaggregates or fine-sized pores (Six et al., 1998; Negassa et al., 2015). Increased lipid abundance may also be due to increased microbial biomass associated with larger, more connected pores (Strong et al., 2004; Huygens et al., 2005). Another explanation for differences in the molecular complexity of C between different pore-size domains is negative enrichment, in which the simpler compounds were preferentially decomposed first, leaving behind chemically complex compounds (Atagana et al., 2002). However, our test of the decomposability of these C compounds by select microorganisms clearly shows that these compounds are not only readily decomposable, but also that their decomposition resulted in greater losses of C as respiration than did the decomposition of the C dissolved in larger pore waters. Thus, it is unlikely that chemical complexity explains the difference in C decomposability in the different pore sizes. More experiments that target the spatial distribution of SOC and microorganisms throughout the soil matrix are needed to develop new, probabilistic models of C stability in soils.

4.2. Microbial metabolism of pore water associated C

Microbial access to soluble C is a significant constraint to overall decomposition. Under unsaturated conditions, even if soils are "moist," many of these fine pores are spatially isolated, resulting in the persistence of C in those locations (Killham et al., 1993). We suggest that C persistence is controlled in part by the degree of hydrologic connectivity within micro- and macropore networks, and the constraints posed by differences in pore throat diameter (Bouckaert et al., 2013). When soil moisture is increased, and pores become hydrologically connected, C protected in the fine pores may solubilize and diffuse to new locations, rendering this C available to local, relatively sessile microorganisms (Wolfaardt et al., 1994). Other researchers observed that substrate availability is more important than microbial metabolism in controlling decomposition rates of SOC (Ruamps et al., 2013).

Our approach sought to focus on the intrinsic decomposability of the soluble C in the absence of the complex soil habitat, therefore rather than to attempt to place different bacteria within the soil matrix as others have done (Ruamps et al., 2013), we used the extracted pore waters as our growth media in *in vitro* incubations. We tested the ability of three model soil microorganisms to decompose the SOC in pore waters to assess the degree to which chemical composition controls C metabolism. All three organisms were competent to decompose the SOC in pore waters within the first 48 h of incubation indicating that colocation of the microbe with substrate is a the limiting factor; the evidence for decomposition observed in the CO_2 fluxes are not clearly coupled to the chemical profiles reported before and after incubation. Therefore, the majority of the SOC processing likely affected the unnamed and unclassified chemical features, suggesting that greater research into this fraction is needed. The metabolic processes we inferred supports this as these are the features within which we saw evidence of transformation in the mass difference analysis.

Our observation of the rapid and extensive decomposition of pore water C by the model fungus *Trichoderma reesei* suggests that the physical protection of soil C could also be compromised by local microbial growth habit for some pore throat diameters; hyphal extension allows soil fungi to exploit new locations in the soil. The

Table 5
Mean and standard error microbial pathways identified with Fourier Transform Ion Cyclotron Resonance (FT-ICR), i.e. of most common mass differences and their corresponding metabolic reactions pooled by pore size class (suction), or inoculae. All metabolic reactions which represent the loss or gain of an amino acid are listed below significantly differed by pore water suction and/or inoculae (shown by lowercase letters). Table only reports 6 identified microbial transformations out of the 46 that differed by pore water suction. Letters not shared within rows indicate significant mean differences calculated using Student's mean comparison test. Inoculants *C. japonicus*, *S. cellulosae* and *T. reseei* stand for *Cellvibrio japonicus*, *Streptomyces cellulosae* and *Trichoderma reseei*, respectively.

Amino Acid	Pore Water Suction		Inoculae			
	−1.5 kPa	- 15 kPa	Control	*C. japonicus*	*S. cellulosae*	*T. reseei*
Alanine	0.36 ± 0.03*	0.27 ± 0.03	0.30 ± 0.06	0.26 ± 0.04	0.32 ± 0.04	0.38 ± 0.04
Asparagine	0.30 ± 0.02*	0.21 ± 0.03	0.19 ± 0.05 b	0.25 ± 0.02 ab	0.25 ± 0.05 ab	0.33 ± 0.03 a
Glycine	0.37 ± 0.03*	0.29 ± 0.02	0.36 ± 0.03	0.25 ± 0.02	0.31 ± 0.06	0.4 ± 0.04
Isoleucine	0.29 ± 0.04*	0.20 ± 0.04	0.34 ± 0.06 a	0.14 ± 0.03 b	0.14 ± 0.06 b	0.35 ± 0.05 a
Leucine	0.29 ± 0.04*	0.20 ± 0.04	0.34 ± 0.06 a	0.14 ± 0.03 b	0.14 ± 0.06 b	0.35 ± 0.05 a
Lysine	0.26 ± 0.02**	0.17 ± 0.03	0.15 ± 0.04	0.19 ± 0.03	0.24 ± 0.04	0.27 ± 0.04
Methionine	0.22 ± 0.03*	0.12 ± 0.02	0.15 ± 0.03	0.17 ± 0.04	0.15 ± 0.04	0.21 ± 0.05
Serine	0.31 ± 0.03**	0.21 ± 0.03	0.29 ± 0.04 ab	0.22 ± 0.04 bc	0.18 ± 0.05 c	0.35 ± 0.03 a
Hydrogenation_Dehydrogenation	2.25 ± 0.04*	2.34 ± 0.04	2.37 ± 0.03 a	2.06 ± 0.04 b	2.32 ± 0.05 a	2.42 ± 0.04 a
Transamination	0.53 ± 0.03**	0.42 ± 0.03	0.33 ± 0.05 b	0.53 ± 0.04 a	0.51 ± 0.04 a	0.54 ± 0.04 a

*$p < 0.05$, **$p < 0.005$.

typical diameter of soil fungal hyphae is 3–6 μm (Six et al., 2006), supporting the hypothesis that fungi have a competitive advantage in exploiting new territories/resources, and may be particularly active in microaggregates (53-25 μm (Kong et al., 2011)), but they are still unable to access fine pores in which more aromatic and condensed forms of C may occur, unlike bacteria (Smith et al., 2014). Therefore, more aromatic and condensed C is being retained in the finest soil pores because fungi are unable to access and mineralize this C (Strong et al., 2004).

Greater microbial transformations involving amino acids observed in coarse pore domains (i.e. the more loosely held pore waters, −1.5 kPa) could also be explained by differences in microbial community composition and function between pores of different sizes and connectivity (Strong et al., 2004; Ruamps et al., 2011; Negassa et al., 2015). Microbial use of alanine, for example, is highest in gram-negative bacteria compared to gram-positive or anaerobic bacteria, and fungi (Apostel et al., 2013) and gram-negative bacteria have been shown to inhabit macroaggregates and coarse pores (Ruamps et al., 2011; Smith et al., 2014) that may have more recent inputs of litter and plant-SOM, their preferred substrate (Kramer and Gleixner, 2008). This is consistent with the higher transformations of alanine and other amino acids observed in coarse pores, which are often more connected than fine pores (Negassa et al., 2015).

What is the source of the soluble C in the different pores? The chemical effects of wetting and drying on SOC accessibility may be key controls. Fine pores are likely to be characterized by finer minerals; the mineral clay fraction is associated with enrichment of N-containing compounds, as well as phenols and lignin monomers. The solubilization and transport of these sorbed materials may drive our observations (Schulten and Leinweber, 1993). The mineral components of the soil pores sorb C compounds under drier soil conditions that are thus at higher local ionic strengths at the pore-scale. Then when water tension decreases, and the pores fill with water, ionic strength decreases and patterns of sorption-desorption associated with different chemical forms of C change (Aubry et al., 2013). Specifically, under low ionic strengths, complex compounds such as polysaccharides bind very strongly and hydrophobic moieties bind very loosely; in contrast, under high ionic strengths, polysaccharides bind loosely and hydrophobic compounds bind more strongly, perhaps due to compression of the double layer (Aubry et al., 2013). This phenomenon would be less frequent, but possibly more significant in affecting net C mineralization, in finer pores subject to spatial isolation under conditions of partial saturation than in coarser, better connected pores in which local hydration varies more regularly (Yang et al., 2013, 2015). Moreover, both fungi and bacteria are likely to more easily access the C in the coarser pores. As these microbes proliferate, then die, their necromass (e.g., cell envelope fragments that may include polysaccharides and other compounds of varying complexity) is released and may be stabilized in soils; recent observations suggest that such bacterial residues are increasingly abundant in soils that age, suggesting that this necromass accumulates as part of the native organic matter pool (Mouvenchery et al., 2016).

5. Conclusions

Our research continues to pose the question, what controls the quality of C in these different pore size domains? We have demonstrated that in these soils i) the soluble C in finer pore domains is nominally more complex (i.e., aromatic and condensed) than the soluble C in coarser pore domains, and ii) the more complex C in the fine pore domains is not recalcitrant, and its decomposition leads to greater losses of C through respiration than the simpler C in coarser pore domains, which suggests that accessibility, or physical protection, is a dominant mechanism for the preservation of C in these soils (Dungait et al., 2012). The pore-size controls on SOC chemistry reported here are based on a small number of samples, although the relationship summarized in (i) above, was consistently observed in all depths of cores drawn from three different locations at this site. What remains to be discovered is if such relationships can be extended to other soils, other sandy soils, or if this is a feature unique to this particular ecosystem.

Our observation of enriched soluble biomolecules, lipids, proteins, and carbohydrates in coarser pore waters may reflect this microbial turnover, a precedent to further decomposition. As these necromass fragments decompose, soluble metabolites may diffuse to finer, more protected pores where they are isolated under drier conditions when soil pores are not hydrologically connected.

Given the heterogeneous distribution of specialized decomposers throughout the soil, the metabolism or persistence of soil C compounds are highly dependent on short-distance transport processes (Ekschmitt et al., 2008). It may be that the non-preferred soil spaces, where microbial activities are absent, slow, or interrupted, are key to understanding the long-term preservation of C in soil (Ekschmitt et al., 2008). Our findings agree with this hypothesis, and we further propose that soils that experience repeated cycles of drying and wetting may result in patterns of CO_2 fluxes that are best predicted using more dynamic representations of C pools, ones that consider i) the transport of C from protected pools into active, ii) the chemical quality of the potentially soluble C, and iii) the type of microorganisms most likely to metabolize this C.

Such a representation could provide a powerful framework for building a new generation of more robust and mechanistic models of SOC dynamics and decomposition.

Acknowledgements

This research is based on work supported by the U.S. Department of Energy, Office of Science, Biological and Environmental Research as part of the Terrestrial Ecosystem Sciences Program. The Pacific Northwest National Laboratory is operated for DOE by Battelle Memorial Institute under contract DE-AC05-76RL01830. A portion of this research was performed using EMSL, a DOE Office of Science user facility sponsored by the Department of Energy's Office of Biological and Environmental Research and located at Pacific Northwest National Laboratory. The authors thank C.R. Hinkle (University of Central Florida) who facilitated access to DWP and whose lab assisted in soil sampling. The authors also thank K. Todd-Brown for her help in developing an R package that processes FT-ICR data and R. Clayton, A. Crump, C. McLean, and K.A. Rod for laboratory analyses.

Appendix A. Supplementary data

Supplementary data related to this article can be found at http://dx.doi.org/10.1016/j.soilbio.2016.11.025.

References

Apostel, C., Dippold, M., Glaser, B., Kuzyakov, Y., 2013. Biochemical pathways of amino acids in soil: assessment by position-specific labeling and 13 C-PLFA analysis. Soil Biology and Biochemistry 67, 31–40.
Atagana, H.I., Haynes, R.J., Wallis, F.M., 2002. Batch culture enrichment of indiginous soil microorganisms capable of catabolizing creosote components. Water Air and Soil Pollution 141, 233–246.
Aubry, C., Gutierrez, L., Croue, J.P., 2013. Coating of AFM probes with aquatic humic and non-humic NOM to study their adhesion properties. Water Research 47, 3109–3119.
Bailey, V.L., Bilskis, C.L., Fansler, S.J., McCue, L.A., Smith, J.L., Konopka, A., 2012. Measurements of microbial community activities in individual soil macroaggregates. Soil Biology & Biochemistry 48, 192–195.
Bailey, V.L., Fansler, S.J., Stegen, J.C., Mccue, L.A., 2013a. Linking microbial community structure to beta-glucosidic function in soil aggregates. Isme Journal 7, 2044–2053.
Bailey, V.L., McCue, L.A., Fansler, S.J., Boyanov, M.I., DeCarlo, F., Kemner, K.M., Konopka, A., 2013b. Micrometer-scale physical structure and microbial composition of soil macroaggregates. Soil Biology & Biochemistry 65, 60–68.
Birch, H., 1958. The effect of soil drying on humus decomposition and nitrogen availability. Plant and Soil 10, 9–31.
Bouckaert, L., Sleutel, S., Van Loo, D., Brabant, L., Cnudde, V., Van Hoorebeke, L., De Neve, S., 2013. Carbon mineralisation and pore size classes in undisturbed soil cores. Soil Research 51, 14–22.
Breitling, R., Ritchie, S., Goodenowe, D., Stewart, M.L., Barrett, M.P., 2006. Ab initio prediction of metabolic networks using Fourier transform mass spectrometry data. Metabolomics 2, 155–164.
Carson, J.K., Gonzalez-Quinones, V., Murphy, D.V., Hinz, C., Shaw, J.A., Gleeson, D.B., 2010. Low pore connectivity increases bacterial diversity in soil. Applied and Environmental Microbiology 76, 3936–3942.
Chassé, A.W., Ohno, T., Higgins, S.R., Amirbahman, A., Yildirim, N., Parr, T.B., 2015. Chemical force spectroscopy evidence supporting the layer-by-layer model of organic matter binding to iron (oxy) hydroxide mineral surfaces. Environmental science & technology 49, 9733–9741.
Chowdhury, N., Marschner, P., Burns, R., 2011. Response of microbial activity and community structure to decreasing soil osmotic and matric potential. Plant and Soil 344, 241–254.
Darrouzet-Nardi, A., Weintraub, M.N., 2014. Evidence for spatially inaccessible labile N from a comparison of soil core extractions and soil pore water lysimetry. Soil Biology & Biochemistry 73, 22–32.
Dungait, J.A., Hopkins, D.W., Gregory, A.S., Whitmore, A.P., 2012. Soil organic matter turnover is governed by accessibility not recalcitrance. Global Change Biology 18, 1781–1796.
Ekschmitt, K., Kandeler, E., Poll, C., Brune, A., Buscot, F., Friedrich, M., Gleixner, G., Hartmann, A., Kastner, M., Marhan, S., Miltner, A., Scheu, S., Wolters, V., 2008. Soil-carbon preservation through habitat constraints and biological limitations on decomposer activity. Journal of Plant Nutrition and Soil Science 171, 27–35.
Fenn, J.B., Mann, M., Meng, C.K., Wong, S.F., Whitehouse, C.M., 1989. Electrospray ionization for mass-spectrometry of large biomolecules. Science 246, 64–71.
Franklin, R.B., Mills, A.L., 2003. Multi-scale variation in spatial heterogeneity for microbial community structure in an eastern Virginia agricultural field. Fems Microbiology Ecology 44, 335–346.
Franklin, R.B., Mills, A.L., 2009. Importance of spatially structured environmental heterogeneity in controlling microbial community composition at small spatial scales in an agricultural field. Soil Biology & Biochemistry 41, 1833–1840.
Huygens, D., Boeckx, P., Van Cleemput, O., Oyarzún, C., Godoy, R., 2005. Aggregate and soil organic carbon dynamics in South Chilean Andisols. Biogeosciences 2, 159–174.
Jastrow, J.D., Amonette, J.E., Bailey, V.L., 2007. Mechanisms controlling soil carbon turnover and their potential application for enhancing carbon sequestration. Climatic Change 80, 5–23.
Killham, K., Amato, M., Ladd, J., 1993. Effect of substrate location in soil and soil pore-water regime on carbon turnover. Soil Biology and Biochemistry 25, 57–62.
Kong, A.Y.Y., Scow, K.M., Cordova-Kreylos, A.L., Holmes, W.E., Six, J., 2011. Microbial community composition and carbon cycling within soil microenvironments of conventional, low-input, and organic cropping systems. Soil Biology & Biochemistry 43, 20–30.
Kramer, C., Gleixner, G., 2008. Soil organic matter in soil depth profiles: distinct carbon preferences of microbial groups during carbon transformation. Soil Biology and Biochemistry 40, 425–433.
Kujawinski, E.B., Behn, M.D., 2006. Automated analysis of electrospray ionization Fourier transform ion cyclotron resonance mass spectra of natural organic matter. Analytical Chemistry 78, 4363–4373.
LaRowe, D.E., Van Cappellen, P., 2011. Degradation of natural organic matter: a thermodynamic analysis. Geochimica et Cosmochimica Acta 75, 2030–2042.
Lawrence, C.R., Neff, J.C., Schimel, J.P., 2009. Does adding microbial mechanisms of decomposition improve soil organic matter models? A comparison of four models using data from a pulsed rewetting experiment. Soil Biology and Biochemistry 41, 1923–1934.
Lehmann, J., Kinyangi, J., Solomon, D., 2007. Organic matter stabilization in soil microaggregates: implications from spatial heterogeneity of organic carbon contents and carbon forms. Biogeochemistry 85, 45–57.
Manzoni, S., Porporato, A., Schimel, J.P., 2008. Soil heterogeneity in lumped mineralization-immobilization models. Soil Biology & Biochemistry 40, 1137–1148.
Marshall, T.J., Holmes, J.W., 1996. Soil Physics, third ed. Cambridge University Press, Cambridge.
Minor, E.C., Steinbring, C.J., Longnecker, K., Kujawinski, E.B., 2012. Characterization of dissolved organic matter in Lake Superior and its watershed using ultrahigh resolution mass spectrometry. Organic Geochemistry 43, 1–11.
Moorhead, D.L., Sinsabaugh, R.L., 2006. A theoretical model of litter decay and microbial interaction. Ecological Monographs 76, 151–174.
Mouvenchery, Y.K., Miltner, A., Schurig, C., Kästner, M., Schaumann, G.E., 2016. Linking atomic force microscopy with nanothermal analysis to assess micro-spatial distribution of material characteristics in young soils. Journal of Plant Nutrition and Soil Science 179, 48–59.
Moyano, F.E., Manzoni, S., Chenu, C., 2013. Responses of soil heterotrophic respiration to moisture availability: an exploration of processes and models. Soil Biology and Biochemistry 59, 72–85.
Negassa, W.C., Guber, A.K., Kravchenko, A.N., Marsh, T.L., Hildebrandt, B., Rivers, M.L., 2015. Properties of soil pore space regulate pathways of plant residue decomposition and community structure of associated bacteria. PLoS one 10, e0123999.
Parker, S.S., Schimel, J.P., 2011. Soil nitrogen availability and transformations differ between the summer and the growing season in a California grassland. Applied Soil Ecology 48, 185–192.
Ruamps, L.S., Nunan, N., Chenu, C., 2011. Microbial biogeography at the soil pore scale. Soil Biology and Biochemistry 43, 280–286.
Ruamps, L.S., Nunan, N., Pouteau, V., Leloup, J., Raynaud, X., Roy, V., Chenu, C., 2013. Regulation of soil organic C mineralisation at the pore scale. Fems Microbiology Ecology 86, 26–35.
Schmidt, M.W., Torn, M.S., Abiven, S., Dittmar, T., Guggenberger, G., Janssens, I.A., Kleber, M., Kögel-Knabner, I., Lehmann, J., Manning, D.A., 2011. Persistence of soil organic matter as an ecosystem property. Nature 478, 49–56.
Schulten, H.R., Leinweber, P., 1993. Influence of the mineral matrix on the formation and molecular composition of soil organic matter in a long-term, agricultural experiment. Biogeochemistry 22, 1–22.
Six, J., Elliott, E.T., Paustian, K., Doran, J.W., 1998. Aggregation and soil organic matter accumulation in cultivated and native grassland soils. Soil Science Society of America Journal 62.
Six, J., Frey, S.D., Thiet, R.K., Batten, K.M., 2006. Bacterial and fungal contributions to carbon sequestration in agroecosystems. Soil Science Society of America Journal 70, 555–569.
Sleighter, R.L., Hatcher, P.G., 2007. The application of electrospray ionization coupled to ultrahigh resolution mass spectrometry for the molecular characterization of natural organic matter. Journal of Mass Spectrometry 42, 559–574.
Smith, A.P., Marín-Spiotta, E., de Graaff, M.A., Balser, T.C., 2014. Microbial community structure varies across soil organic matter aggregate pools during tropical land cover change. Soil Biology and Biochemistry 77, 292–303.
Steduto, P., Cetinkoku, O., Albrizio, R., Kanber, R., 2002. Automated closed-system canopy-chamber for continuous field-crop monitoring of CO_2 and H_2O fluxes. Agricultural and Forest Meteorology 111, 171–186.
Strong, D.T., De Wever, H., Merckx, R., Recous, S., 2004. Spatial location of carbon decomposition in the soil pore system. European Journal of Soil Science 55,

739–750.
Stutter, M.I., Lumsdon, D.G., Cooper, R.J., 2007. Temperature and soil moisture effects on dissolved organic matter release from a moorland Podzol O horizon under field and controlled laboratory conditions. European Journal of Soil Science 58, 1007–1016.
Tfaily, M.M., Chu, R.K., Tolic, N., Roscioli, K.M., Anderton, C.R., Pasa-Tolic, L., Robinson, E.W., Hess, N.J., 2015. Advanced solvent based methods for molecular characterization of soil organic matter by high-resolution mass spectrometry. Analytical Chemistry 87, 5206–5215.
Wolfaardt, G.M., Lawrence, J.R., Robarts, R.D., Caldwell, D.E., 1994. The role of interactions, sessile growth, and nutrient amendments on the degradative efficiency of a microbial consortium. Canadian Journal of Microbiology 40, 331–340.
Yang, X., Liu, C., Fang, Y., Hinkle, R., Li, H., Bailey, V.L., Bond-Lamberty, B., 2015. Simulations of ecosystem hydrological processes using a unified multi-scale model. Ecological Modelling 296, 93–101.
Yang, X., Liu, C., Shang, J., Fang, Y., Bailey, V.L., 2013. A unified multi-scale model for pore-scale flow simulations in soils. Soil Science Society of America Journal 78, 108–118.